## **PROCEEDINGS OF SPIE**

SPIEDigitalLibrary.org/conference-proceedings-of-spie

# Multiparameter solid phantom for fluorescence imaging standardization

Maria Anastasopoulou
Dimitris Gorpas
Maximilian Koch
Pilar Beatriz Garcia-Allende
Uwe Klemm
Angelos Karlas
Vasilis Ntziachristos



### Multiparameter solid phantom for fluorescence imaging standardization

Maria Anastasopoulou<sup>a,b</sup>, Dimitris Gorpas<sup>a,b</sup>, Maximilian Koch<sup>a,b</sup>, Pilar Beatriz Garcia-Allende<sup>a,b</sup>, Uwe Klemm<sup>a</sup>, Angelos Karlas<sup>a,b</sup>, Vasilis Ntziachristos<sup>a,b,\*</sup>

<sup>a</sup> Helmholtz Zentrum München, Institute for Biological and Medical Imaging, Ingolstädter Landstraße 1, Neuherberg, Germany; <sup>b</sup> Technical University Munich, Chair for Biological Imaging, Arcisstraße 21, Munich, Germany

#### **ABSTRACT**

Despite recent advances in fluorescence imaging, standardization of systems remains an unmet need. We developed a new comprehensive phantom that resolves multiple system parameters simultaneously and could be used for system performance comparison.

Keywords: Fluorescence imaging, standardization, phantoms, benchmarking, multiparameter, intraoperative

#### 1. INTRODUCTION

Interventional fluorescence imaging serves as a promising modality for surgical guidance in malignant tissue excisions, offering better malignancy delineation and improving the prognosis for recurrent and residual disease emergence [1]. The arrival of new fluorescent agents that target specific disease moieties has made fluorescence imaging even more attractive due to the increased sensitivity, specificity and contrast of the diseased tissue over the healthy one [2].

The wide range of fluorescence intraoperative systems in different research facilities and clinics leads to the need for benchmarking of the different systems and evaluation of their performance. This major issue of standardization and system calibration can be addressed by the development of specific fluorescence phantoms that mimic tissue optical properties. This type of phantoms should be made from a base material that provides a fixed shape and not allows shape deformation over time. Moreover, the fluorescent agent should be photostable over time and over different environmental conditions. These two requirements make polyurethane [3] the best choice for base material and equivalently Quantom dots (Qdots) [4] for fluorescent agent. Currently, there have been developed some dedicated phantoms that mostly examine either camera sensitivity [5], or excitation light leakage into the fluorescence camera channel [6] or the effect of fluorochrome depth on fluorescent signal [7]. So, they address only a single or few system specifications. Therefore, there is a need for a new class of phantoms that can assess simultaneously multiple parameters. All these parameters should be examined simultaneously and not by the use of different phantoms, so that the optimal parameters for the best tradeoff between all the system specifications can be achieved.

Here we present a comprehensive solid polyurethane phantom that can assess simultaneously multiple system parameters, such as the camera sensitivity, fluorescence intensity variations as a function of optical properties and depth, illumination homogeneity, resolution and cross talk from excitation light leaking into the fluorescence channel.

\*v.ntziachristos@tum.de

Clinical and Preclinical Optical Diagnostics, edited by J. Quincy Brown, Ton G. van Leeuwen, Proc. of SPIE-OSA Vol. 10411, 104110J · © 2017 OSA-SPIE CCC code: 1605-7422/17/\$18 · doi: 10.1117/12.2286059

Proc. of SPIE-OSA Vol. 10411 104110J-1

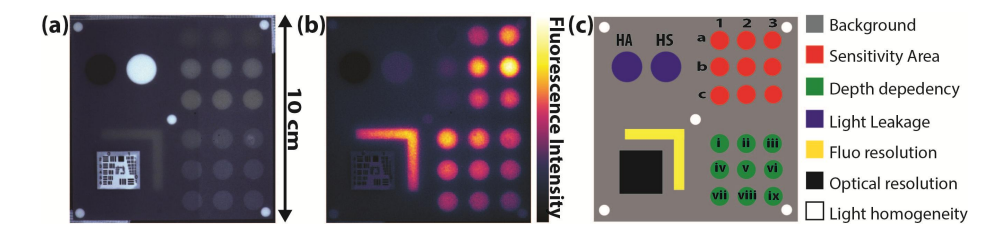


Figure 1: a) Color image of the phantom, b) Fluorescence image of the phantom and c) Schematic of the phantom: HA: high absorbing area, HS: high scattering area. 1,2,3: increasing Fluorescence and absorption. a,b,c: increasing scattering. From i to ix: increasing depth from the surface

#### 2. MATERIALS AND METHODS

The phantom, with dimensions  $10x10x2.2 \text{ cm}^3$ , is depicted on Figure 1. Fig.1a shows the color image of it, whereas Fig.1b the fluorescence. In Fig.1c, we can see an overview of the different system specification groups. The phantom is made of transparent rigid polyurethane (WC-783 A/B, BJB Enterprises, Tustin) and contains different structures for assessing the different system specifications. The phantom was fabricated by molding a cuboid of the background material as it is depicted on Fig.2. The background (Gray area on Fig.1c) absorption is imparted by alcohol soluble nigrosin (Sigma Aldrich, St. Louis), whereas the background scattering by TiO<sub>2</sub> particles (Titanium IV Oxide, Sigma Aldrich, St. Louis). The absorption coefficient was set to 0.5 cm<sup>-1</sup> at 750 nm and the reduced scattering coefficient to 10 cm<sup>-1</sup> at 750 nm. The scattering of the structures on the phantom is induced by hemin (Sigma Aldrich, St. Louis), while Qdots (800-nm; Thermofisher Scientific, Waltham) with emission at 800 nm are used as a fluorescence agent. After the filling and curing of the background block (Fig.2a), different specification examination structures were drilled on the surface (Fig.2b). Afterwards, the openings were filled with the appropriate amounts of hemin, TiO<sub>2</sub> and Qdots (Fig.2c). Then, the different depths in the depth structure were milled (Fig.2d) and filled with the background material (Fig.2e). Finally, the upper surface was trimmed and polished (Fig.2f). All the structures on the phantom were made 12 mm deep.

The structure that interrogates the sensitivity and the fluorescence intensity variation as a function of optical properties consists of nine 10-mm diameter wells array (Red area on Fig.1c). Absorption concentration varies across the columns (20, 20 and 40 μg/g Hemin for 1,2,3 in Fig.1c) and scattering across the rows (0.33, 0.66 and 1 μg/g TiO<sub>2</sub> for a,b,c in Fig.1c). Fluorescence varies across the columns (1, 5 and 10 nM Qdots for 1,2,3 in Fig.1c). The depth related structure consists again of nine 10-mm diameter wells array (Green area on Fig.1c), all of them having the same fluorescence concentration of 10 nM Qdots and same optical properties (20 µg/g Hemin and 0.66µg/g TiO<sub>2</sub>). The fluorescent cylindrical wells are embedded at varying depths within the phantom and specifically at 0.2, 0.4, 0.6, 0.8, 1, 1.33, 1.66, 2, and 3, mm (from i to ix structure in Fig.1c) below the phantom surface. The area of light leakage examination (Blue area on Fig.1c) comprises a 15-mm diameter well of very high absorption (3.74 mg/g nigrosin) and one of very high scattering (10 mg/g TiO<sub>2</sub>). Regarding the resolution part, the lower left quadrant tests for the optical and diffusive resolution. A standard 1951 United States Air Force resolution test chart (USAF, Black area on Fig.1c) is fixed on the top of the phantom for the characterization of the white light optical resolution. Moreover, an L-shaped fluorescence structure (Yellow area on Fig.1c) with 0.66 mg/g TiO<sub>2</sub>, 20 µg/g Hemin and 10 nM Qdots is employed for the examination of photon diffusion and fluorescence resolution. The dimensions of the L shape are 30 mm x 30 mm with 5 mm width of each branch. Finally, for the evaluation and correction of the homogeneity of the light illumination, there are five 5 mm diameter identical reflective (10 mg/g TiO<sub>2</sub>) wells (White area on Fig.1c) dispersed on the phantom's surface.

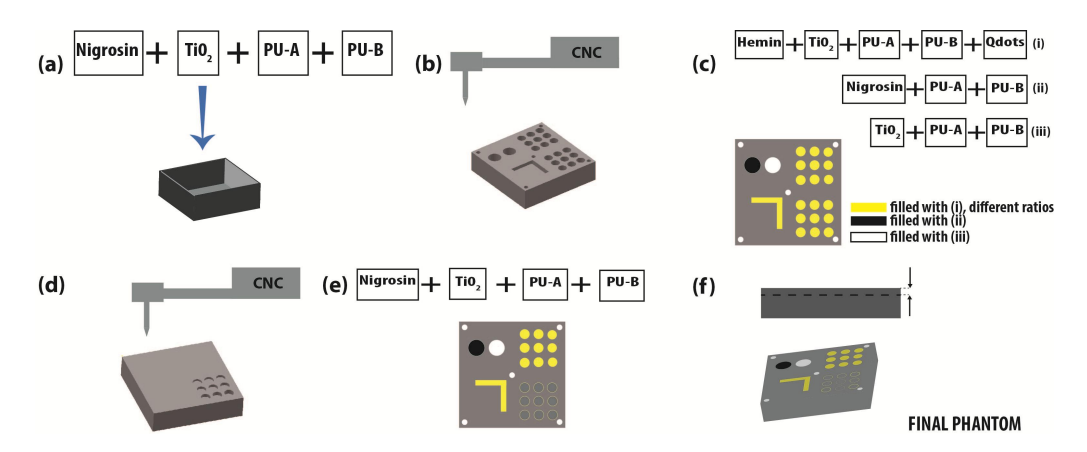


Figure 2: Phantom development process: a) Background block filling, b) Drilling of the wells, c) Filling of the wells, d) Drilling different depths for the depth structure, e) Fill the depth structure wells with the background material and f) Trim and polish the final phantom.

#### 3. RESULTS

The specifications that can be tested with the phantom can be used to compare different systems to each other, to configure the optical working specifications of one system or to evaluate the system's performance over time. Different metrics can be applied in order to interpret the parameters and get quantitative information. Here, we present a simple comprehensive way with applying cross sections to the entities of the fluorescence image to get a first impression of parameters' assessment.

Regarding the light leakage (Fig.3b), the cross section of the two wells can be used to estimate the light leakage signal as a metric for the evaluation of the filter light rejection. The higher the signal the worse the cross talk. Another metric would be the ratio of the light leakage measurement over the reflected light of the color camera in Fig.1a.

System sensitivity (Fig.3c) can be assessed by observing the fluorescence levels, for example by cross section of the sensitivity structure of the fluorescence image, for the different fluorophore concentration wells. Moreover, for the same concentration of Qdots, the different effect of optical properties variation can be assessed and an evaluation of algorithms for fluorescence intensity quantification can be performed.

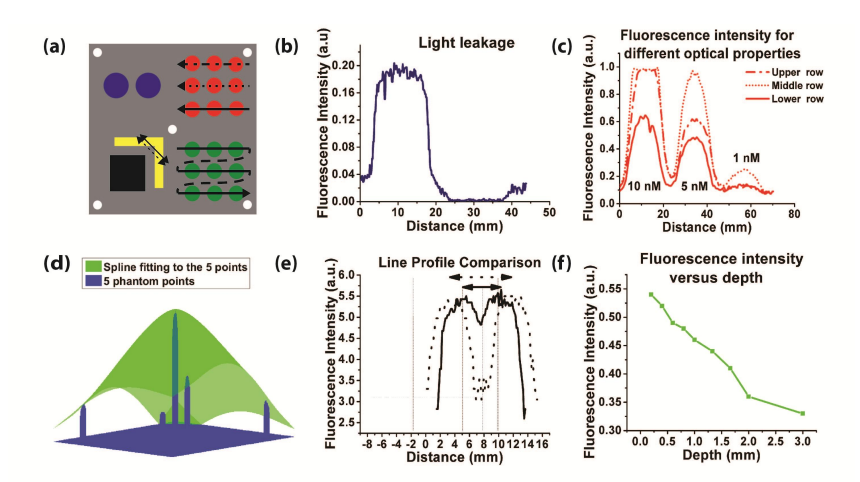


Figure 3: a) Depth structure of the phantom. b) Fluorescence intensity versus the depth distance and c) Five spots fluorescence profile and comparison of the five reflective spots surface profile with the surface profile of a white reflectance sheet.

The 3D profile of the five reflective wells placed in the center and at the corners of the phantom can be used as a quick estimation for white light illumination homogeneity. Moreover, using five sampling points a three dimensional surface (Fig. 3d) that approximates the illumination field can be used to perform flat field correction.

The USAF chart on the phantom can be employed to estimate optical resolution, based on the quantification of the contrast transfer function. Although the L-shape entity has been manufactured to have sharp borders, they are imaged blurred due to photon diffusion. This makes this element ideal for estimating the fluorescence resolution and/or assess the performance of systems with diffusion correction capabilities. One metric to test different fluorescence resolutions would be the distance from the inner vertex of L shape structure that the two branches of the L shape start to be resolved. In Fig.3e, we see how the two L branches start to be unresolved as we get closer to the inner vertex.

The performance of cameras that account for depth-related fluorescence signal variations can be assessed through the depth entity on the phantom using plots that depict the fluorescence signal versus the varying depth (Fig. 3f).

#### 4. CONCLUSION

The phantom described herein can serve as a comprehensive tool for the evaluation of a system's performance and for the comparison between systems of markedly different specifications. Different utilizations of the described parameters, that can be assessed simultaneously, render this phantom a flexible solution for system benchmarking. In the future, such complex phantoms could be used for system assessment in an automatic way through a single snapshot.

#### REFERENCES

- [1] M. Koch and V. Ntziachristos, "Advancing Surgical Vision with Fluorescence Imaging," no. October 2015, pp. 1–12, 2016.
- [2] W. Scheuer, G. M. van Dam, M. Dobosz, M. Schwaiger, and V. Ntziachristos, "Drug-Based Optical Agents: Infiltrating Clinics at Lower Risk," Sci. Transl. Med., vol. 4, no. 134, p. 134ps11-134ps11, 2012.
- [3] M. L. Vernon, J. Freachette, Y. Painchaud, S. Caron, and P. Beaudry, "Fabrication and characterization of a solid polyurethane phantom for optical imaging through scattering media," Appl. Opt., vol. 38, no. 19, pp. 4247–4251, 1999.
- [4] U. Resch-Genger, M. Grabolle, S. Cavaliere-Jaricot, R. Nitschke, and T. Nann, "Quantum dots versus organic dyes as fluorescent labels," Nat. Methods, vol. 5, no. 9, pp. 763–775, 2008.
- [5] B. Zhu, J. C. Rasmussen, and E. M. Sevick-Muraca, "A matter of collection and detection for intraoperative and noninvasive near-infrared fluorescence molecular imaging: to see or not to see?," Med. Phys., vol. 41, no. 2, p. 22105, 2014.
- [6] B. Zhu, I.-C. Tan, J. C. Rasmussen, and E. M. Sevick-Muraca, "Validating the sensitivity and performance of near-infrared fluorescence imaging and tomography devices using a novel solid phantom and measurement approach," Technol. Cancer Res. Treat., vol. 11, no. 1, pp. 95–104, 2012.
- [7] M. Roy, A. Kim, F. Dadani, and B. C. Wilson, "Homogenized tissue phantoms for quantitative evaluation of subsurface fluorescence contrast.," J. Biomed. Opt., vol. 16, no. 1, p. 16013, 2011.